ICOMP
Lewis Research Center
Ohio Aerospace
Institute

Navier-Stokes Analysis of the Flowfield Characteristics of an Ice Contaminated Aircraft Wing

J. Chung
Institute for Computational Mechanics in Propulsion
Lewis Research Center, Cleveland, Ohio

Y. Choo, A. Reehorst, M. Potapczuk, and J. Slater
Lewis Research Center, Cleveland, Ohio

National Aeronautics and
Space Administration

Lewis Research Center

January 1999

Navier-Stokes Analysis of the Flowfield Characteristics of an Ice Contaminated Aircraft Wing

Joongkee Chung
Institute for Computational Mechanics in Propulsion / Ohio Aerospace Institute
NASA Lewis Research Center
Cleveland, Ohio

Yung Choo, Andrew Reehorst, Mark Potapczuk and John Slater
NASA Lewis Research Center
Cleveland, Ohio

Abstract

An analytical study was performed as part of the NASA Lewis support of a National Transportation Safety Board (NTSB) aircraft accident investigation. The study was focused on the performance degradation associated with ice contamination on the wing of a commercial turbo-prop-powered aircraft. Based upon the results of an earlier numerical study conducted by the authors[1], a prominent ridged-ice formation on the subject aircraft wing was selected for detailed flow analysis using 2-dimensional(2-D), as well as, 3-dimensional(3-D) Navier-Stokes computations. This configuration was selected because it caused the largest lift decrease and drag increase among all the ice shapes investigated in the earlier study. A grid sensitivity test was performed to find out the influence of grid spacing on the lift, drag, and associated angle-of-attack for the maximum lift ($C_{l_{max}}$). This study showed that grid resolution is important and a sensitivity analysis is an essential element of the process in order to assure that the final solution is independent of the grid.

The 2-D results suggested that a severe stability and control difficulty could have occurred at a slightly higher angle-of-attack(AOA) than the one recorded by the Flight Data Recorder (FDR)[2]. This stability and control problem was thought to have resulted from a decreased differential lift on the wings with respect to the normal loading for the configuration. The analysis also indicated that this stability and control problem could have occurred whether or not natural ice shedding took place.

Numerical results using an assumed 3-D ice shape showed an increase of the angle at which this phenomena occurred of about 4 degrees. As it occurred with the 2-D case, the trailing edge separation was observed but started only when the AOA was very close to the angle at which the maximum lift occurred.

Nomenclature

MVD	Median Volume Diameter (in μm)
LWC	Liquid Water Content (in g/m^3)
CPS	Control Point Smoothing
CFD	Computational Fluid Dynamics
IGES	Initial Graphics Exchange Specifications
LW	Left Wing
RW	Right Wing
NTSB	National Transportation Safety Board
FDR	Flight Data Recorder
IRT	Icing Research Tunnel (at NASA Lewis)
AOA	Angle-of-Attack, Degrees
B-B	Badwin-Barth Turbulence Model
S-A	Spalart-Allmaras Turbulence Model
C_l	2-Dimensional Lift Coefficient
$C_{l_{max}}$	Maximum 2D Lift coefficient
C_L	3-Dimensional Lift Coefficient
C_d	2-Dimensional Drag Coefficient
C_D	3-Dimensional Drag Coefficient
y_1	Distance from the wing surface to the first grid point in normal direction (minimum wall spacing)
y^+	Reynolds number based on the typical velocity and length scales for the turbulence

Introduction

Aircraft performance degradation due to ice contamination remains a concern within the aviation industry. Recent accidents and incidents have shown that undetected ice accretion or ineffective ice removal methods can lead to altered performance characteristics and sudden loss of stability and control, with the potential for the most severe consequences[3]. As part of a response to a request for technical assistance by

the NTSB, the NASA Lewis Icing Branch has used simulation methods to examine the possibility of ice contamination being a contributing factor in an accident involving a commercial turbo-prop powered aircraft. This examination involved tests in the Icing Research Tunnel (IRT) at NASA Lewis to obtain the ice shapes which would have accreted under the flight conditions of the accident aircraft[1,2] followed by a numerical analysis effort to determine the possible performance degradation associated with those ice shapes, which is the subject of this paper. Because of higher than normal turbulence levels, partly due to the existence of the heat exchanger and spray bars necessary for icing cloud generation, the IRT is not considered the best facility for post-ice-accretion aero-measurement. High fidelity aeroperformance data is thus obtained from other wind tunnel facilities. However, due to constraints of cost and of available time associated with model fabrication and for extensive wind tunnel tests, Computational Fluid Dynamics (CFD) was considered an alternative means of providing post-ice-accretion aeroperformance analysis.

An earlier numerical study by the authors[1], aimed at building a foundation for flow analysis of iced airfoils, attempted to define the iced surface as closely as possible to the original geometry in order to make the numerical grid generation and simulation process accurate and efficient. That study showed that, for similar ice accretion times, an ice formation with a prominent ridge caused the most severe performance degradation compared to other ice shapes having only sharp bumps of similar sizes. Based on this information and the flight conditions recorded by the FDR[2], a numerical study was performed to determine if the degraded aerodynamics resulting from such an ice contamination could have led to the type of control upset attributed to the accident aircraft.

Approach

Ice Shape Modeling and Grid Generation

The first step in the study was the modeling of the ice shapes obtained in the IRT[4]. An ice shape with a ridge on the upper surface near the leading edge and a number of small bumps on the lower surface (Fig. 1a & 1b) was obtained in the IRT at the mid-section of a vertically mounted (Fig 1c) wing. At the centerline of this 6 foot test model, the airfoil was roughly a NACA 23015 and the chord length was about 68 inches. The icing spray conditions which produced this ice shape were a median volume diameter (MVD) of $20\mu m$, a total temperature of $26°F$, an angle-of-attack of $5°$, a liquid water content (LWC) of $0.8 g/m^3$ and a 5 minute spray time.

Among the ice shapes numerically tested, the prominent leading edge ridged-ice caused the most significant performance degradation. The height of the ridge is less than 1% of the chord (0.0074c). An ice shape of this size would have been hard to see by the pilots in the cockpit. The geometry shown in fig. 1a has several sharp corners and high curvature segments. Curve discretization and eventual generation of a quality field grid on this geometry were time consuming. A mathematical model for systematic surface smoothing was presented in reference 1. This approach was implemented in an interactive code, TURBO-GRD[5] to generate surface shapes with different smoothing levels. It constructs a smooth curve whose shape is controlled by a piece-wise linear curve formed by selected discretized points. These points are called control points (CPs) as they control the shape of the curve they construct. A brief summary of this process is presented here.

1) The digitized ice shape data is first read in and one CP is assigned to each digitized point.

2) A curve is constructed using these CPs. The discretized data points are moved onto the new smoothed curve determined by the CPs. The points are then redistributed at equally spaced intervals along the curve. The number of discretized data points on the iced segment is unchanged by this process. We will call this a baseline curve or a curve with 100% Control Point Smoothing (CPS).

3) Using this baseline curve as a starting point, the number (or percentage) of CPs can be reduced, thus generating curves with various levels of smoothness. During this process, the shape and the number of points in the un-iced areas do not change.

The current study showed that a 50% level of CPS or higher is required to adequately represent the ice shapes as measured by having marginal influence (i.e. less than 5% variation) on the resulting lift and drag values. All grid generation was performed using the commercial code GRIDGEN[7].

The 2-D grids used in this study for modeling the region around the iced airfoil are composed of two blocks where the inner and outer blocks have an overlapping interface between 0.5c and 0.6c (c=chord) from the airfoil surface. The inner block had a C-type grid with a wake cut downstream of the trailing edge and a much denser distribution of grid points than the outer block. Both blocks had downstream boundary set at 15.0c from the leading edge. (Fig. 2a and 2b) The C-type grid was also used for the outer block with the farfield boundaries placed at a distance of 15 chord lengths from the body surface in all directions. This method of constructing 2-block grids allowed for easier control of

the grid generation process and better quality of the resulting grid, especially near the complex iced surfaces.

Flow solver and boundary conditions

A general purpose Reynolds averaged Navier-Stokes flow analysis code, NPARC[7] was used for the simulation. In NPARC, the Navier-Stokes equations are formulated as central-difference approximations with added artificial dissipation and are solved using an approximate-factorization scheme which results in a scalar penta-diagonal matrix for steady state computations. Complex geometries can generally be handled with ease by the multi-block capability and modular boundary conditions. Inviscid, laminar, and turbulent flows can be simulated for 2-D (or axi-symmetric) and 3-D geometries. A capability to calculate the lift and drag was added to a subroutine for this analysis. The code also has Runge-Kutta and implicit subiteration schemes for time accurate computations. For the simulation of turbulent flows, NPARC offers algebraic, one-equation, and two-equation turbulence models. In this study, both the Spalart-Allmaras[8] and the Baldwin-Barth[9] one-equation turbulence models were used. At the far field boundary, a non-reflecting type boundary condition was applied.

Grid Sensitivity Test

In the abscence of detailed measurement data of the pressure or velocity fields, grid sensitivity tests can be used to determine the optimum grid density. In order to develop the highest quality simulation of aerodynamic properties of interest, such as lift, $C_{l_{max}}$ and drag, a series of grids (for the inner block) having different resolutions in both normal and stream-wise (circumferential) directions were constructed (the outer block was fixed with the dimension of 115 x 20). The NPARC code was then run, using these grids, and the aerodynamic quantities of interest were compared. For this grid sensitivity test, the Spalart-Allmaras turbulence model was chosen for its known robustness in airfoil/wing calculations. Examples of the importance of grid sensitivity testing and how grid properties can affect the simulation results, especially at high AOA, can be found in Ref. 10 and 11.

The first set of grids constructed (Table 1) was used for an investigation of the normal direction sensitivity, which was followed by a study on the effect of minimum wall spacing (y1) (Table 2) and finally by a study of the effect of packing grid points in the stream-wise direction (Table 3). In tables 1 and 3, 's' represents the stream-wise direction and 'n' represents the normal direction respectively.

Figure 3a shows that the lift values obtained using the s1n1 grid varied by over 10% from those obtained using the s1n2 grid. On the other hand, the lift values changed only 0.26 - 2.21% when it was refined to the level of s1n3 grid (detailed numerical values can be found in table 4). A similar trend was observed for drag values as indicated in Fig. 3b and table 4. This suggests that the n1s1 grid did not have a sufficient number of points to predict the maximum lift value while showing that any further refinement beyond the level of the s1n2 grid was not necessary. This led to a further investigation of the effect of minimum wall spacing on aerodynamic performance parameters (see Table 2).

Another purpose of the second study was to find an appropriate value of y1 to be used for 3-D grid generation which would allow efficient and fast convergence while not sacrificing accuracy. Throughout this study, the computations were performed until the L2-residual dropped at least 3 to 4 orders of magnitude and the lift value changed by less than 10^{-7}.

In this second step of the analysis, all aspects of the grid except the value of y1 were fixed. Using the w1 grid as a baseline, the y1 value was either decreased or increased to investigate the effect on the lift. Figure 4 and Table 5 show that the increase of y1 from 2.0 x 10^{-6} to 5.0 x 10^{-6} resulted in 0.27 - 1.36% change in the lift value below 9 degree AOA but resulted in a 4.53% increase at 11 degree AOA. In the case of decreased y1 (w3 grid), a similar trend was noted except that it resulted in a reduction of the lift by 0.29 ~ 2.16% up to an AOA of 9 degrees and a drop of 6.91% at 11 degree AOA. An investigation of the y^+ values showed that the average value of y^+ was approximately 2.7 for the w2 grid, 1.0 for the w1 grid and less than 1.0 for the w3 grid respectively. This result shows that the AOA for the maximum lift was predicted for all three grids as 9 degrees and that some difference existed in the computations at the 11 degree AOA. From this study, it was decided to use a y1 of 2.0 x 10^{-6} for the 2-D studies. For the 3-D study, a y1 of 5.0 x 10^{-6} was used for the grid generation to minimize CPU time.

To draw the final conclusion on the choice of proper grid resolution, a stream-wise (circumferential) direction grid sensitivity test was performed using the three grids listed in table 3. In this case, only the stream-wise point density was changed to determine its effect on the aerodynamic performance parameters.

As Fig. 5 and table 6 show clearly, there was less than a 1% change in the lift values regardless of the resolution. Changes in the drag were less than 1% except at the higher AOAs for the s3n2 grid (1.58% maximum). From this test,

we decided to use the dimension of 350 x 50 with the y1 value of 2.0 x 10^{-6} as the base line.

2-dimensional grids used for the airfoil with ridged-ice and aileron deflection

According to the FDR, at the time of the NASA-defined control upset, the left aileron deflection was 2.56 degrees down and the right aileron deflection was 2.74 degrees up. This configuration was intended for a right banking movement. The approximate angle-of-attack and Reynolds number were 7.8 degrees and 10 million (based on the chord) respectively. Another greater aileron deflection that occurred after the defined control upset was 7.94 degrees aileron down on the left wing (LW) and 8.26 degrees up on the right wing (RW).

Four grids for the airfoil with ridged-ice accretion, reflecting these four different angles of aileron deflection, were generated using the guidelines developed from the grid sensitivity tests. More grid points were used near the aileron in the stream-wise direction over the grids used in the sensitivity study. Another set of four grids for airfoils without ice but having the same aileron deflection angles were also generated for comparison to the iced airfoils.

3-dimensional grid generation

An IGES-type surface data of the turbo-prop aircraft is pictured in a shaded mode in Fig 6a. The geometry data was obtained from the manufacturer and some assumptions were made to generate the grids for both iced and un-iced wings.

A number of assumptions are worth noting: First, the available data did not have information about the wing tip geometry. Figures 7c-d show the approximated wing tip used in the analysis. Second, as shown in Fig 6b, only the outboard section of the wing (approximately 5.4 m in the span-wise direction) was used for the current analysis. Third, the downward deflected aileron on the left wing (only 2.56 degree deflection angle) was modeled as having no gap with the wing surface in the span-wise direction. This was accomplished by creating a smoothly connected surface shape shown in Fig 7e (see also Fig 7c). The idea behind this was that the existence of a fence on the real aircraft between the aileron and the outboard flap next to it would have prevented any span-wise flow. Fourth, for the modeling of an assumed 3-D ice shape, the height and the shape of the ridged-ice on the upper surface and of the bumps on the lower surface were kept constant (Fig 7a & 7b). They were projected in both span-wise directions from the location where the ice shape data was taken in the IRT (see fig 6b). Since the wing did not have a large sweep angle and the maximum thickness was larger near the root, the root area had a lower collection effi-

ciency. Thus, it was considered to be a plausible assumption to use a constant cross-section ice shape and to smoothly taper it near the wing tip (Fig. 7d).

Figure 7f shows an example of grid lines around the ridge and a typical velocity profile showing separation behind it. Based on the above assumptions, 3-D grids consisting of approximately 400,000 and 1 million grid points in a single-block format were generated for the clean(un-iced) and iced wings with an aileron deflection angle of 2.56 degrees. The symmetry plane was located at z = 4.5 m (z=0 being the fuselage centerline) and the span-wise location of the aileron was between z = 6.3 m and 9.6 m. The 3-D computational results were compared to the 2-D results at the z=6.59 m location where the 2-D IRT ice shape was taken.

Discussion of Results

2-D flow analysis

Aileron deflection # 1 (2.56 down LW, 2.74 up RW)

The figures Fig. 8a - 9b show the lift and drag coefficients versus angle-of-attack obtained by steady state computations using two different one-equation turbulence models, Spalart-Allmaras (S-A)[8] and Baldwin-Barth (B-B)[9]. This calculation was performed to investigate differences in the numerical prediction resulting from the application of these two models. Both figure 8a(S-A) and 9a(B-B) show that the ice caused a slight lift decrease at low AOAs and a further significant decrease at higher angles.

The open circles represent lift values for the un-iced LW with 2.56 degree aileron down and the squares represent those of un-iced RW with 2.74 degree aileron up. We assume that no ice shedding occurred on any of the wings. The lift was computed every 2 degrees between 3 and 15 degrees for the un-iced wings. Without the ice, as the lift curves show, the airplane would not have had any problem banking to the right with the higher lift on the LW. The iced wing computations were done for AOA of 3, 5, 7, 7.8, 9, 10, and 11 degrees (7.8 degree was the AOA where the control problem occurred according to the FDR).

A close examination of the lift change on the iced LW predicted by the S-A turbulence model in Fig 8a shows that the peak value occurred around 9 degrees. The maximum lift was predicted to occur at a slightly lower AOA, (7.8 degrees: Fig 9a), when the B-B model was used. The maximum lift on the iced RW occurred at approximately 10 degrees for the S-A model (Fig 8a) and 9 degrees for the B-B model (Fig

9a). Also noticeable from the two graphs is that a reversal of lift values occur at around 11 degrees and 10.5 degrees respectively. The lift values on each iced-wing become very close at around 10 ~ 10.5 degree AOA and it could have caused difficulty in aileron control.

Now, if we consider the possibility of ice completely shedding off the RW, as was indicated by the experiment in the IRT[4], the reversal of the lift values could occur at a lower angle-of-attack. In this case, 9 (S-A) or 8 (B-B) degrees would be the approximate angles where the reversal would have happened. These are angles fairly close to those recorded by the FDR. Computation for higher than 11 degree angle-of-attack was not attempted because of the expected unsteady nature of the flow.

Figures 8b and 9b show the drag coefficient prediction using the two turbulence models. They indicate a considerable increase in the drag but show no cross-over of the drag values for the iced wings. Both figures indicate that the LW showed consistently higher drag values than the RW. This supports the FDR record that there was a tendency for yaw in the counter-clockwise direction before the accident happened. A little closer examination of the above four graphs also show that the S-A model predicted slightly higher lift and lower drag values than the B-B model. Though different from the current study, a previous computational study[12] using these turbulence models suggests that difference in the spreading rates (or amount of mixing) in the wake regions could be a contributing factor to these differences. Figures 10a-c show the leading edge and trailing edge separation predicted by the S-A turbulence model. The trailing edge separation starts at an AOA of 7 degrees and this separation region grows as the AOA increases. When the AOA reaches 9 degrees, the trailing edge separation covers almost 70% of the upper surface. Figure 11 shows the turbulent viscosity contour at the 9 degree AOA.

Aileron deflection # 2 (down 7.94 LW, up 8.26 RW)

A higher angle aileron input was applied to attempt to bank to the right after the defined control upset. This condition was also simulated using the 2-D Navier-Stokes analysis procedure (Fig 12 - 15b). Unlike the above lower angle setting, the cross-over of lift was not observed, but, a considerable decrease of the lift differential was predicted (Fig 14a and 15a). As it occurred with setting #1, shedding of the ice from the RW would have still caused the lift reversal, at a slightly higher AOA of 10 degrees. However, under aileron setting #2, the effectiveness of the aileron might have been questionable even at lower AOA again raising the possibility of the control dilemma. The S-A turbulence model predicted

higher lift and lower drag values than the B-B model with the exception of the 11 degree AOA case. At this angle, the S-A model predicted a higher value for both lift and drag than the B-B model.

3-D flow analysis

Due to the time requirements for the calculations, the 3-D analysis was limited to only one downward aileron deflection angle of 2.56 degrees on the left wing for both iced and clean cases. This calculation was performed to investigate whether there were any 3-D effects which altered the 2-D flow characteristics. The S-A model was used for all 3-D computations and the results were compared to those of the 2-D computations using the same S-A model.

The 3-D computation showed that the $\alpha_{c_{l,max}}$ occurs at about 13 degrees, approximately 4 degrees higher than the 2-D case. At 9 degree AOA, where the 2-D calculation showed considerable change in the pressure coefficient plot on the upper surface (Fig 16a), the 3-D calculation showed little difference between the clean and the iced wings (Fig 16b). The comparison of the 2-D and 3-D pressure coefficient shows some differences just aft of the ridge and at about 0.6 x/c on the upper surface (Figure 16c). The rake profile and Mach contour plots from the 3-D analysis at an AOA of 13 degrees (Fig 17a & 17b) indicate that no large scale separation occurs near the trailing edge on the upper surface. At 15 degree AOA though, a trailing edge separation starts, as shown in the next series of graphs depicting pressure coefficient (Fig 18), span-wise variation of the pressure along lines parallel to the trailing edge (Fig 19a & 19b), Mach contour (Fig 20a) and velocity profile (Fig 20b). The rake profile at 15 degrees AOA (Fig 21) shows a large separation region on the upper surface as well as circular motion of the fluid parallel to the wing surface. This occurs near the span-wise region where the aileron was deflected. The change of span-wise pressure distribution shown in figure 22 indicates that a small scale trailing edge separation started at an AOA of 13 degrees and intensified at 15 degree AOA. The differences in the lift and in the drag between the clean 3-D wing and the iced 3-D wing are shown in figures 23 and 24. The 3-D lift and drag are defined as

$$C_L = \frac{L}{q_\infty S} \quad \text{and} \quad C_D = \frac{D}{q_\infty S}$$

where q_∞ is dynamic pressure and S represents a reference area (wing span x mean chord) and L and D are total lift and drag of the entire wing respectively. The causes of the

difference between the 2-D and 3-D computations are probably due to one or more of the following.

1) Relatively poor resolution of the 3-D grids.

2) Proportionally smaller ridge height at the inboard section of the wing could prevent the trailing edge separation at the lower AOA. Due to the 3-D nature of the flow, this could affect the flow in the outboard section as well.

3) The smoothly connected surface constructed for the deflected aileron could prevent possible 3-D effects in the span-wise direction.

4) Downwash caused by the tip vortices increase the adverse pressure gradient near the leading edge (Fig 16c) producing an effect analogous to induced camber[13].

Concluding Remarks

The purpose of this study was to perform a post-ice-accretion CFD analysis of the contaminated airfoil/wing surfaces of a turbo-prop aircraft under the reconstructed icing conditions from an accident. This analysis was performed in order to obtain some qualitative trends and to provide insight into the aerodynamics that may have led to a control upset. The grid sensitivity tests which preceded the numerical simulation showed that the prediction of accurate lift and drag values as well as AOA of maximum lift can be affected by the grid resolution. The 2-D analysis indicated that the control upset could have occurred with or without the complete ice shedding at or slightly higher than the angle-of-attack recorded by the FDR. The performance degradation was observed to be a result of a combination of trailing and leading edge separation. In the case of 3-D analysis, the trailing edge separation was observed to start near the maximum lift point. The 3-D results also showed that the maximum lift occurred 4 degrees later than the 2-D case. More work is needed in 3-D ice shape modeling and in grid refinement to understand the differences between the 2-D and 3-D results.

References

1. J. Chung, A. Reehorst, Y. Choo, and M. Potapczuk, "Effect of Airfoil Ice Shape Smoothing on the Aerodynamic Performances", AIAA Paper 98-3242 AIAA/ASME/SAE/ASEE Joint Propulsion Conference, Cleveland, July, 1998

2. "The Group Chairman's Aircraft Performance Study", NTSB Accident #DCA97MA017, 1998

3. "National Transportation Safety Board Aviation Accident Report, In Flight Icing Encounter and Uncontrolled Collision with Terrain, Comair Flight 3272, Embraer EMB-120T, N265CA Monroe, Michigan, January 9, 1997", NTSB Accident #DCA97MA017, 1998

4. A. Reehorst, J. Chung, M. Potapczuk, Y. Choo, W. Wright, and T. Langhals, "An Experimental and Numerical Study of Icing Effects on the Performance and Controllability of a Twin Engine Aircraft", AIAA Paper 99-0374, Reno, NV, Jan., 1999

5. Y. Choo, J. Slater, T. Henderson, C. Bidwell, D. Braun, and J. Chung, "User Manual for Beta Version of Turbo-GRD - A Software System for Interactive Two-Dimensional Boundary/Field Grid Generation, Modification, and Refinement", NASA TM-1998-206631, Oct., 1998

6. J. Chawner and J. Steinbrenner, "Automatic Grid Generation Using GRIDGEN", NASA CP-3291, Surface Modeling, Grid Generation, and Related Issues in CFD Solutions, May 9-11, 1995

7. NPARC Version 3.0 User's Manual, NPARC Alliance, September, 1996

8. P. Spalart and S. Allmaras, "A One-Equation Turbulence Model for Aerodynamic Flows", AIAA Paper 92-0439, Jan. 1992

9. B. Baldwin and T. Barth, "A One-Equation Turbulence Transport Model for High Reynolds number Wall-Bounded Flows", AIAA Paper 91-0610, Jan. 1991

10. S. Rogers, "Progress in High-Lift Aerodynamic Calculations", AIAA Paper 93-0194, Jan., 1993

11. W. Anderson, "Navier-Stokes Computations and Experimental Comparisons for Multi-element Airfoil Configurations", AIAA Paper 93-0645, Jan., 1993

12. S. Rogers, F. Menter, P. Durbin, & N. Mansour, "A Comparison of Turbulence Models in Computing Multi-Element Airfoil Flows", AIAA Paper 94-0291, Jan., 1994

13. E. Polhamus, "A Survey of Reynolds Number and Wing Geometry Effects on Lift Characteristics in the Low Speed Stall Region", NASA Contractor Report 4745, June 1996

Table 1. Grids used for normal direction sensitivity test

grid	dimension of the inner block	minimum wall spacing	# of points in the wake
s1n1	350 x 35	5.0×10^{-6}	40
s1n2	350 x 50	2.0×10^{-6}	40
s1n3	350 x 70	1.0×10^{-6}	40

Table 2. Grids used to investigate the effect of y1

grid	dimension of the inner block	minimum wall spacing	# of points in the wake
w1	350 x 50	2.0×10^{-6}	40
w2	350 x 50	5.0×10^{-6}	40
w3	350 x 50	1.0×10^{-6}	40

Table 3. Grids used for streamwise direction sensitivity test

grid	dimension of the inner block	minimum wall spacing	# of points in the wake
s1n2	350 x 50	2.0×10^{-6}	40
s2n2	391 x 50	2.0×10^{-6}	45
s3n2	335 x 50	2.0×10^{-6}	50

Table 4. Results of grid sensitivity test in normal direction

Effect of normal direction grid spacing on the Lift : Spalart-Allmaras turb. model					
angle-of-attack	grid s1n1	grid s1n2	% diff w.r.t. s1n1	grid s1n3	% diff w.r.t. s1n2
3	0.466902E+00	0.474712E+00	1.67	0.482297E+00	1.60
5	0.656589E+00	0.677035E+00	3.17	0.687467E+00	1.55
7	0.796187E+00	0.844164E+00	6.03	0.846396E+00	0.26
9	0.811387E+00	0.940808E+00	15.95	0.920070E+00	-2.21
11	0.610636E+00	0.881574E+00	44.38	0.896499E+00	1.70
Effect of normal direction grid spacing on the Drag					
angle-of-attack	grid s1n1	grid s1n2	% diff w.r.t. s1n1	grid s1n3	% diff w.r.t. s1n2
3	0.109985E-01	0.111718E-01	-1.55	0.116647E-01	4.39
5	0.144212E-01	0.138728E-01	-3.81	0.141511E-01	2.02
7	0.212905E-01	0.191165E-01	-10.10	0.192776E-01	0.84
9	0.373112E-01	0.292152E-01	-21.68	0.307334E-01	5.17
11	0.836481E-01	0.551994E-0	-34.01	0.556031E-01	0.72

Table 5. Grid sensitivity test by varying the minimum wall spacing

	Effect of y1 spacing on the Lift : Spalart-Allmaras turb. model				
angle-of-attack	grid w1	grid w2	% diff w.r.t.w1	grid w3	% diff w.r.t. w1
3	0.474712E+00	0.476098E+00	0.27	0.473321E+00	-0.29
5	0.677035E+00	0.681638E+00	0.56	0.673610E+00	-0.50
7	0.844164E+00	0.853181E+00	1.07	0.832419E+00	-1.40
9	0.940808E+00	0.953617E+00	1.36	0.920462E+00	-2.16
11	0.881574E+00	0.921539E+00	4.5	0.820662E+00	-6.91
	Effect of y1 spacing on the Drag				
angle-of-attack	grid w1	grid w2	% diff w.r.t.w1	grid w3	% diff w.r.t. w1
3	0.111718E-01	0.111890E-01	0.18	0.112559E-01	0.81
5	0.138728E-01	0.138832E-01	0.07	0.139814E-01	0.79
7	0.191165E-01	0.191050E-01	-0.05	0.193351E-01	1.15
9	0.292152E-01	0.289606E-01	-0.89	0.302606E-01	3.56
11	0.551994E-01	0.526106E-01	-4.69	0.597563E-01	8.26

Table 6. Effect of streamwise direction grid refinement

	Effect of streamwise direction refinement on the Lift : Spalart-Allmaras turb. model				
angle-of-attack	grid s1n2	grid s2n2	% diff w.r.t s1n2	grid s3n2	% diff w.r.t. s2n2
3	0.474712E+00	0.475970E+00	0.25	0.474485E+00	-0.32
5	0.677035E+00	0.680178E+00	0.46	0.681312E+00	0.16
7	0.844164E+00	0.850468E+00	0.75	0.853843E+00	0.39
9	0.940808E+00	0.946762E+00	0.64	0.949348E+00	0.26
11	0.881574E+00	0.877536E+00	-0.47	0.869843E+00	-0.88
	Effect of streamwise direction refinement spacing on the Drag				
angle-of-attack	grid s1n2	grid s2n2	% diff w.r.t s1n2	grid s3n2	% diff w.r.t. s2n2
3	0.111718E-01	0.112136E-01	0.36	0.112155E-01	0.09
5	0.138728E-01	0.139457E-01	0.58	0.139903E-01	0.27
7	0.191165E-01	0.192379E-01	0.63	0.194336E-01	0.99
9	0.292152E-01	0.294111E-01	0.65	0.298083E-01	1.33
11	0.551994E-01	0.555839E-01	0.69	0.564566E-01	1.58
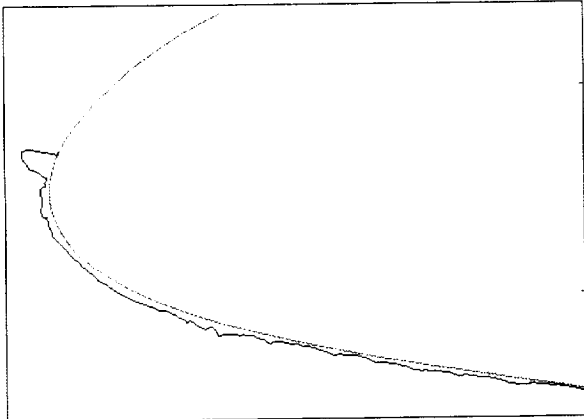
Fig. 1a Ridged-ice formation near the leading edge

Fig. 1b Rough ice shape on the lower side of the turboprop wing - IRT experiment

Fig. 1c Vertically mounted wing in the test section
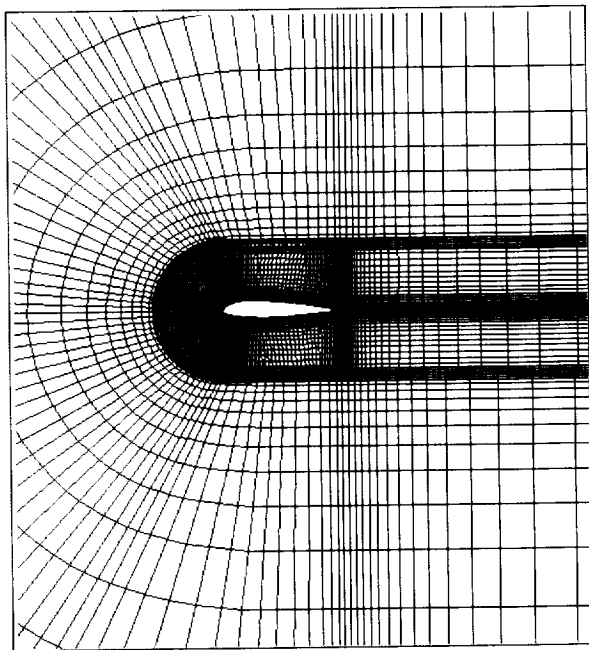
Fig. 2a Two-block grid system used for 2-D analysis
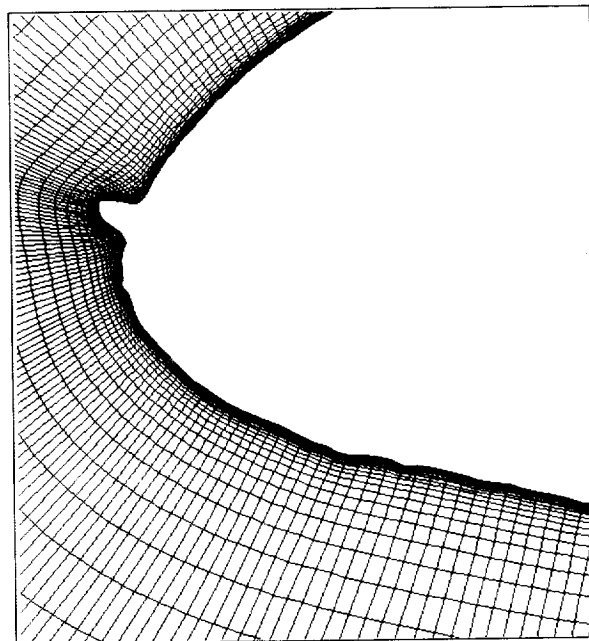
Fig. 2b Detailed grid near the ridged-ice

Fig. 3a   Grid sensitivity test in normal direction

Ridged-ice, S-A turb. model, inner block grid density changes
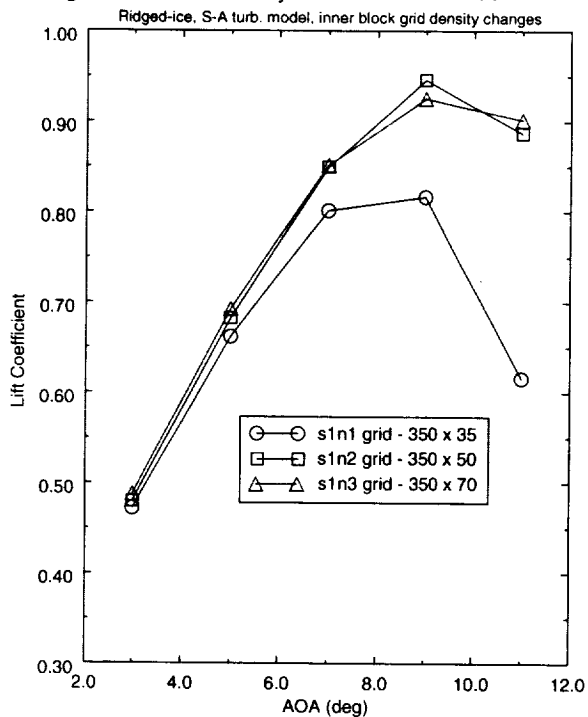
Fi 3. 3b   Grid Sensitivity in Normal Direction

Ridged-ice, S-A turb. model, inner block grid density changes
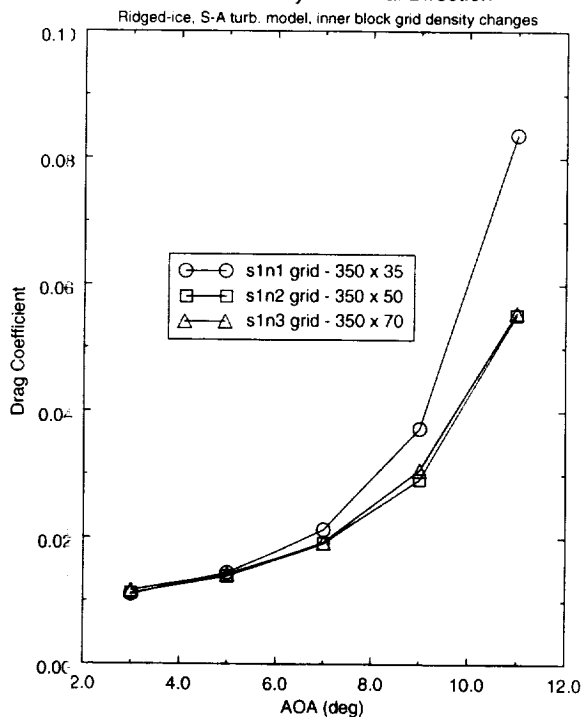
Fig. 4 Grid sensitivity test using minimum wall spacing

Various y1, S-A turb. model used
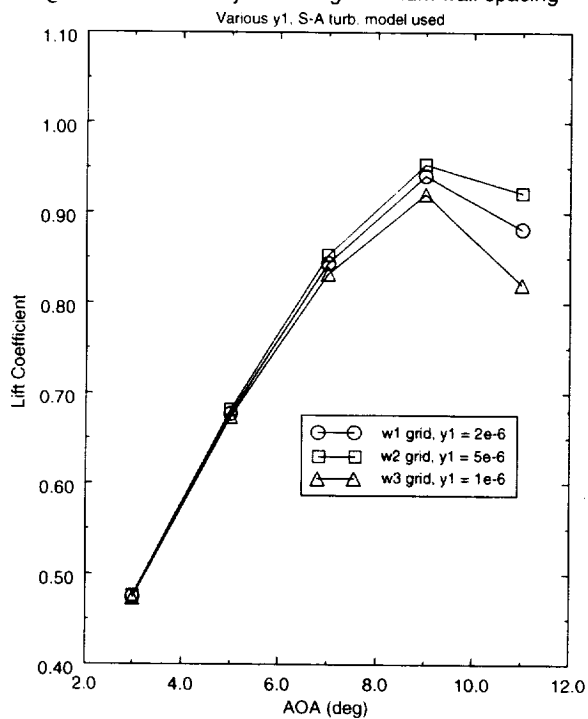
Fig. 5   Streamwise direction grid sensitivity test

Ridged-ice, S-A turb. model, inner block grid density changes
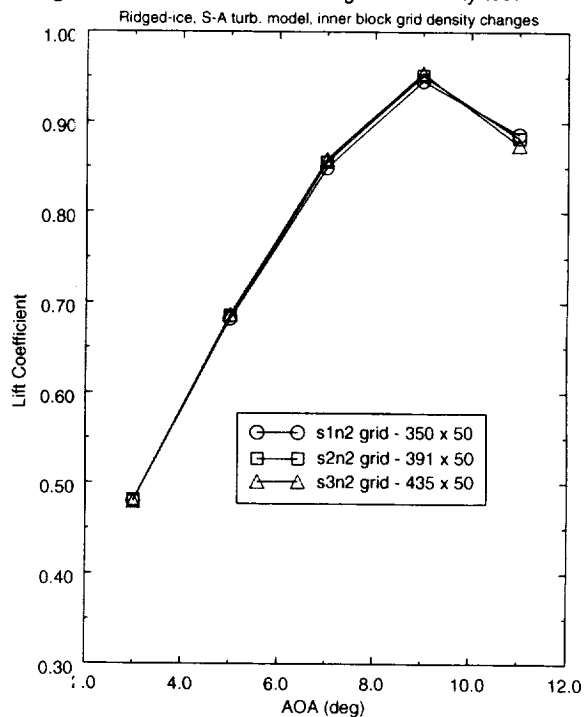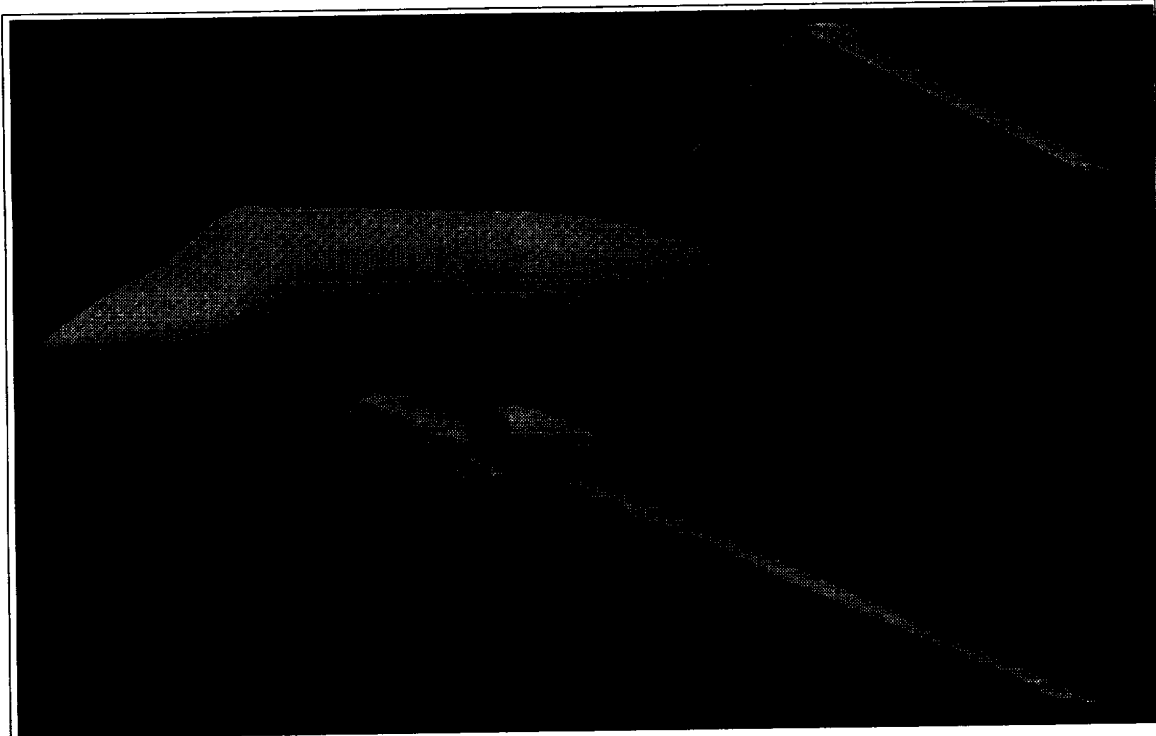
Fig. 6a Overall picture of the turboprop aircraft used for the numerical analysis in a shaded mode
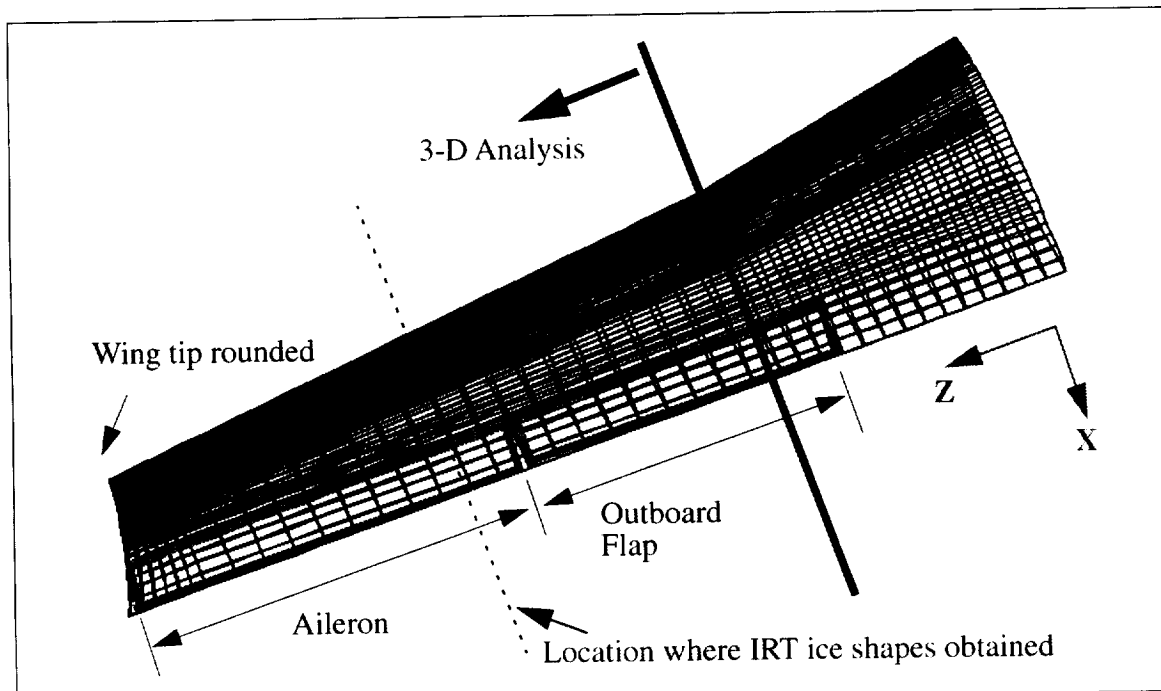
Fig. 6b Three dimensional wing modeling showing the area for numerical analysis
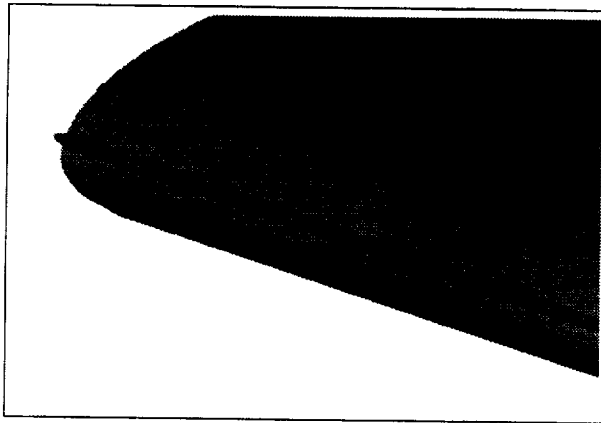
Fig. 7a Ice shape at the LE of the wing
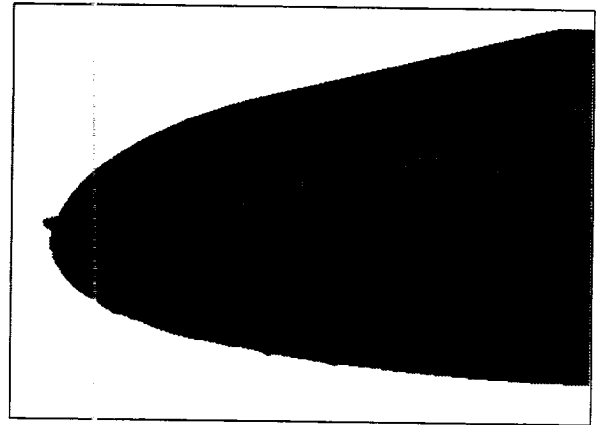
Fig. 7b Ice shape modelling on the lower surface
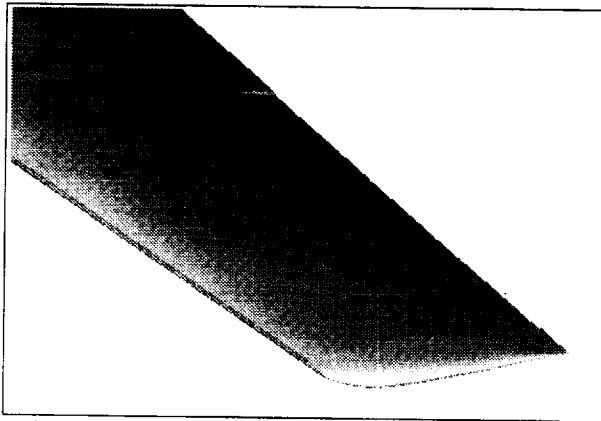
Fig. 7c Aileron and the wing tip
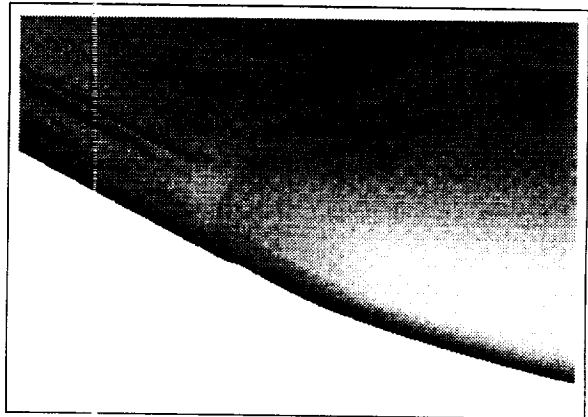
Fig. 7d Tapering ice shape near the simulated
wing tip faring

Wing tip
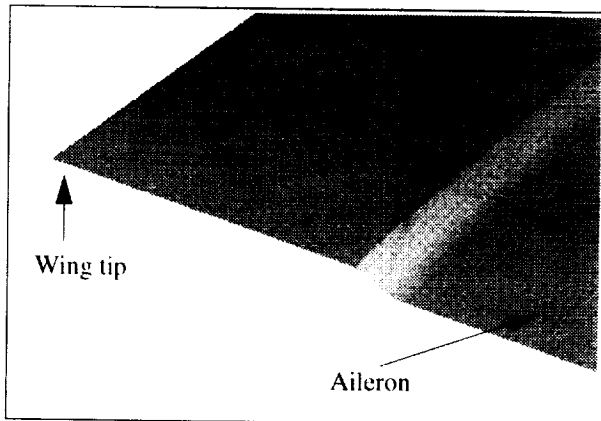
Aileron

Fig. 7e Modelling of the aileron at 2.56 deg. down
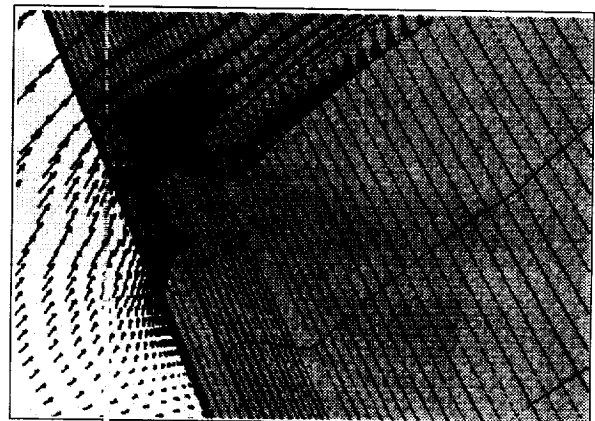
Fig. 7f Grid system at the rideged-ice and the
separation behind it

Fig. 8a Lift Comparison for airfoil with ridged ice, S-A turb. model
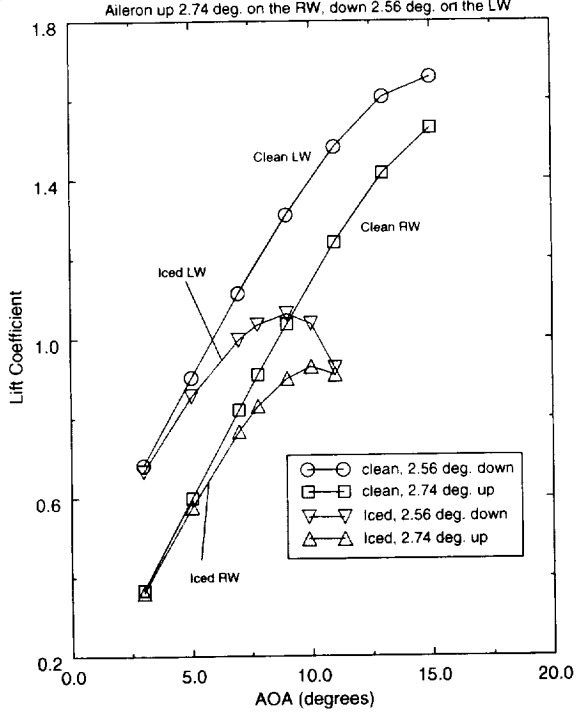
Fig.8b Drag Comparison for airfoil with ridged Ice, S-A turb. model
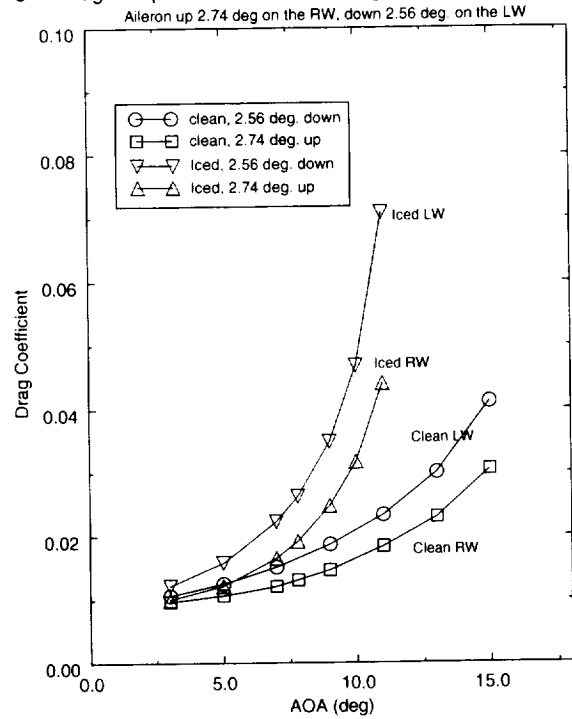
Fig. 9a Lift Comparison for airfoil with ridged ice, B-B turb. model
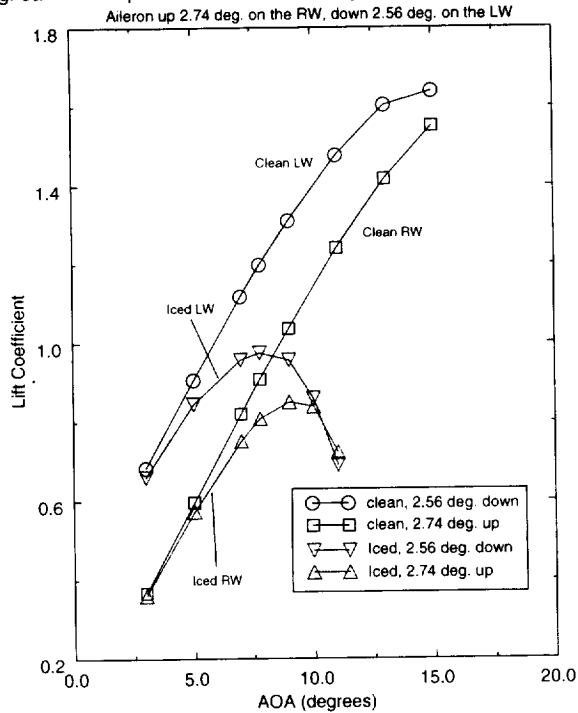
Fig.9b Drag Comparison for airfoil with ridged Ice, B-B turb. model
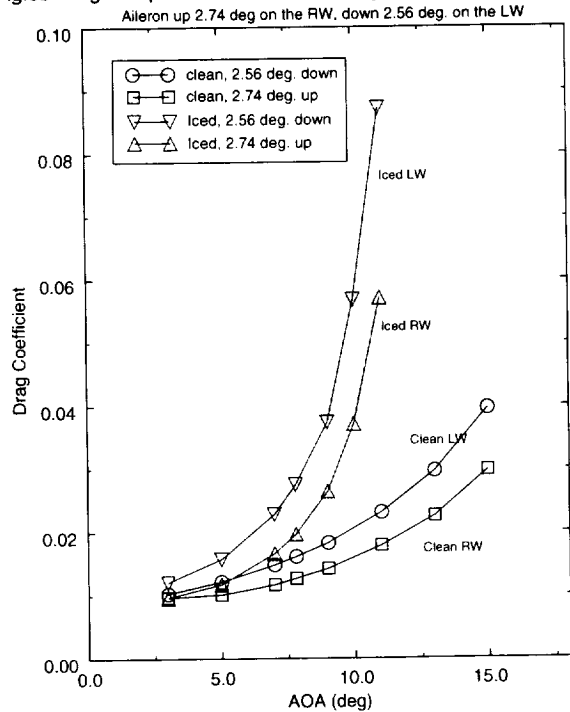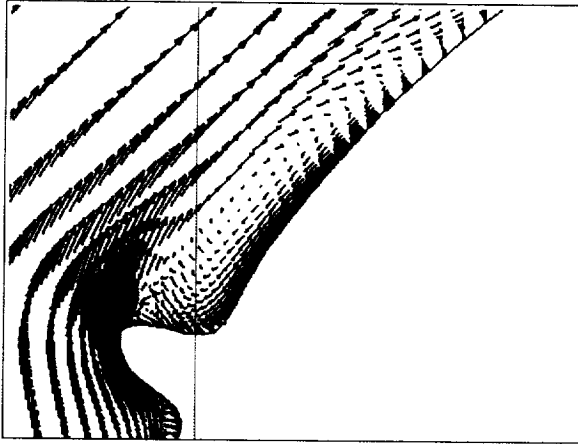
Fig. 10a Seperation aft of the ridged-ice
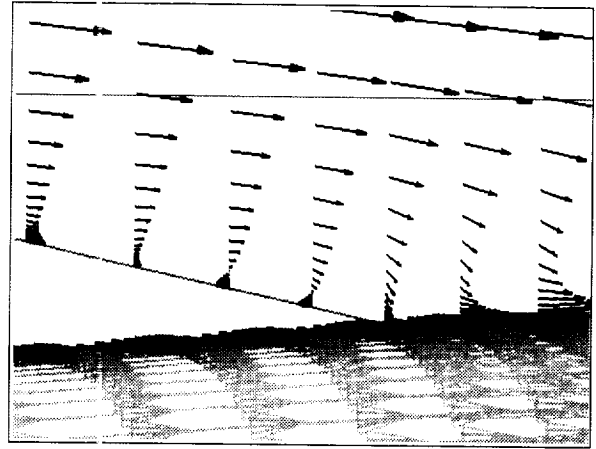
Fig. 10b Trailing Edge separation at AOA = 7 deg.
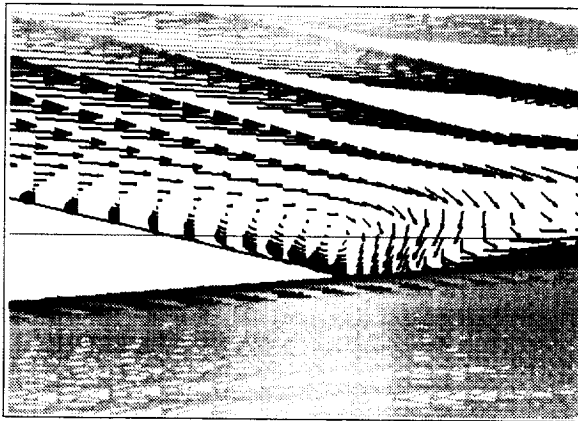
Fig. 10c Increased TE separation at AOA =9
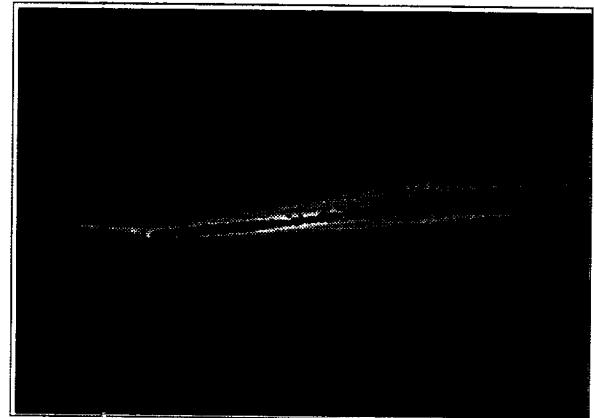
Fig. 11 Turbulent viscosity contour, AOA = 9
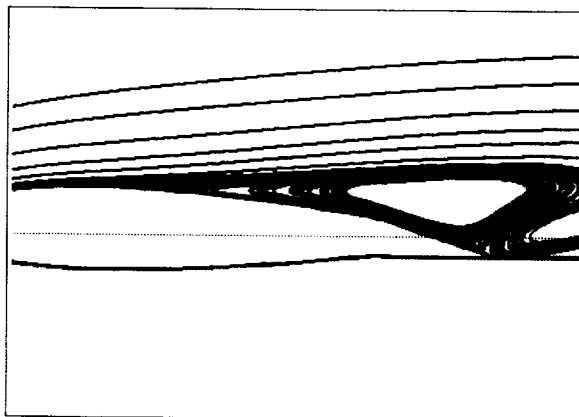
Fig. 12 Large separation near the TE at AOA = 10 degree for 7.94 deg. downward aileron deflection
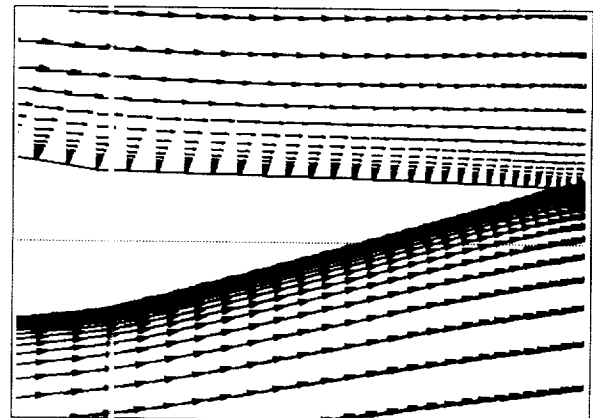
Fig. 13. Velocity profile of the TE of aileron deflected 8.26 deg. upward at AOA = 10 degrees

Fig. 14a Lift Comparison for airfoil with ridged ice, S-A turb. model
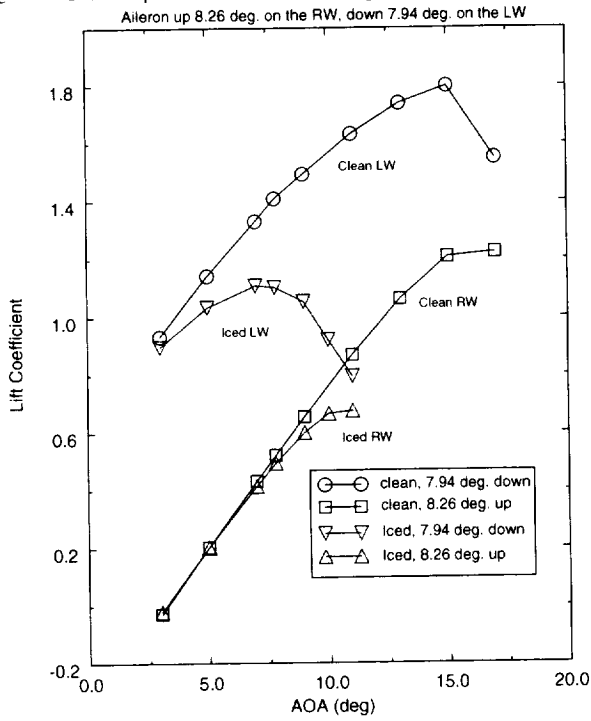
Fig 14b Drag comparison for Ridged-ice case, S-A turb. model
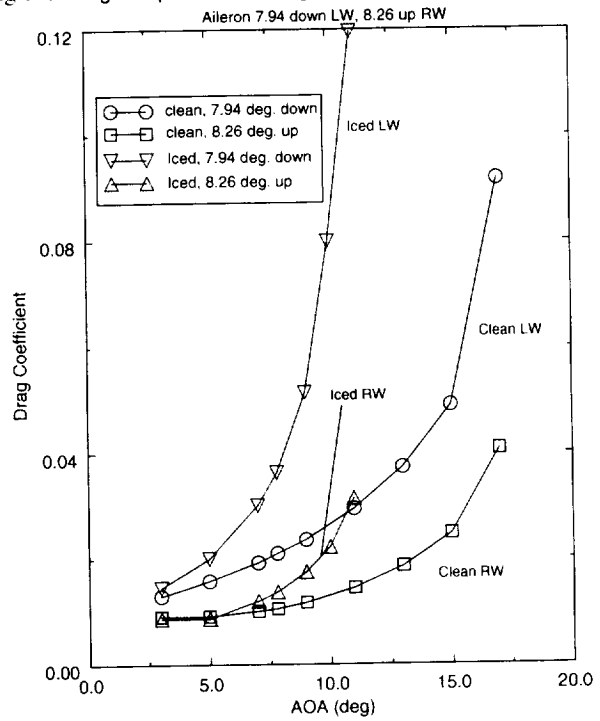
Fig. 15a Lift Comparison for airfoil with ridged ice, B-B turb. model
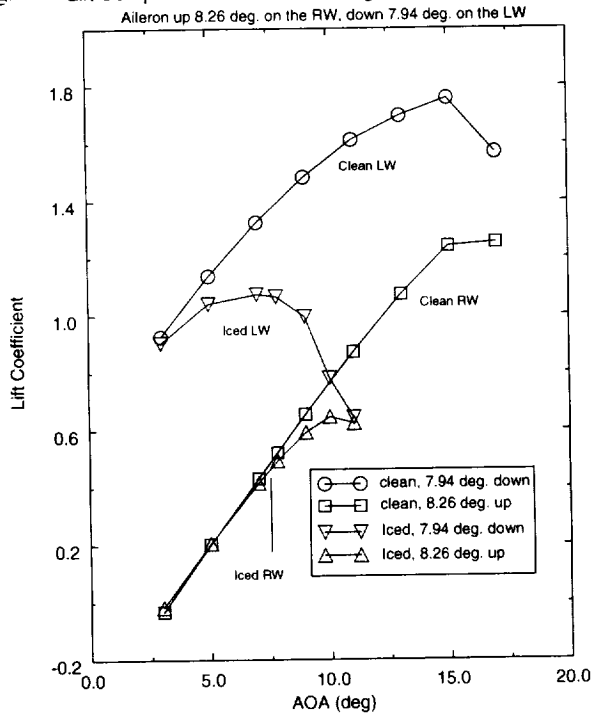
Fig.15b Drag comparison for Ridged-ice case, B-B turb. model
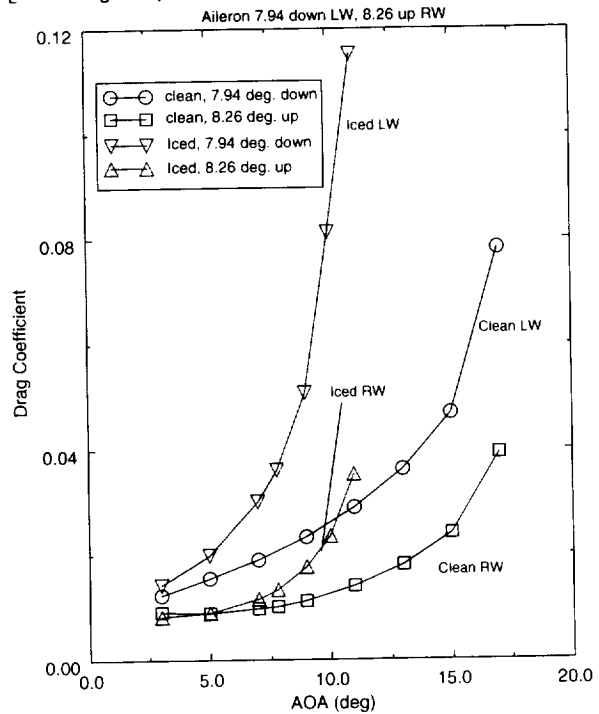
Fig. 16a 2-D Cp comparison between clean & iced airfoils

AOA = 9 deg., aileron 2.56 deg. down LW, S-A turb. model

2-D Clean airfoil
2-D Iced airfoil
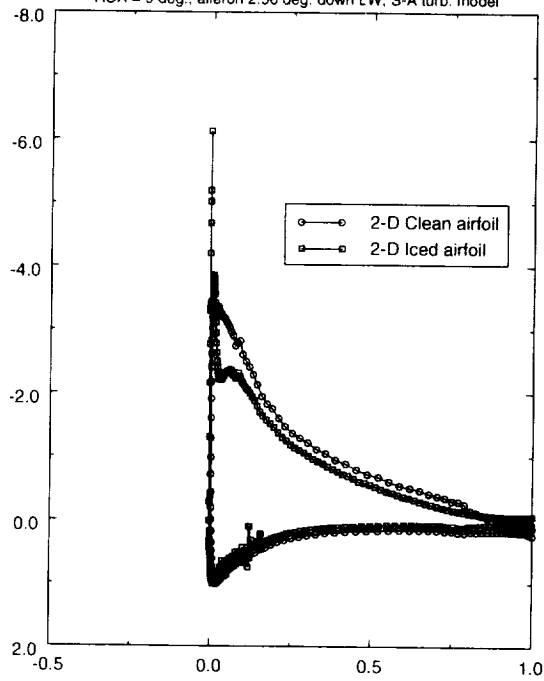
Fig. 16b 3-D Cp comparison between clean & iced wings

AOA = 9 deg. at Z = 6.59 m, aileron 2.56 deg. down LW, S-A model

3-D clean wing
3-D iced wing
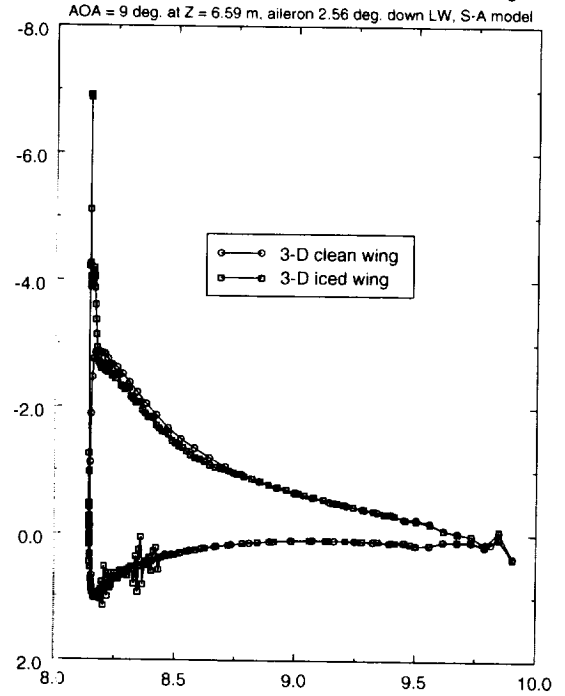
Fig. 16c   2-D & 3-D Cp comparison at AOA = 9 deg.

Iced wing with aileron 2.56 deg. down, LW, S-A turb. model

2-D iced airfoil
3-D iced wing at z = 6.59 m
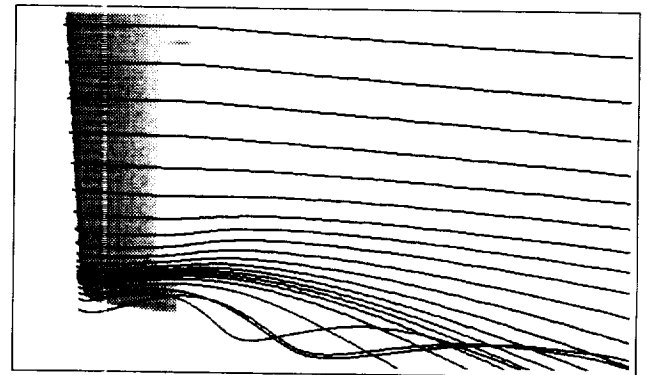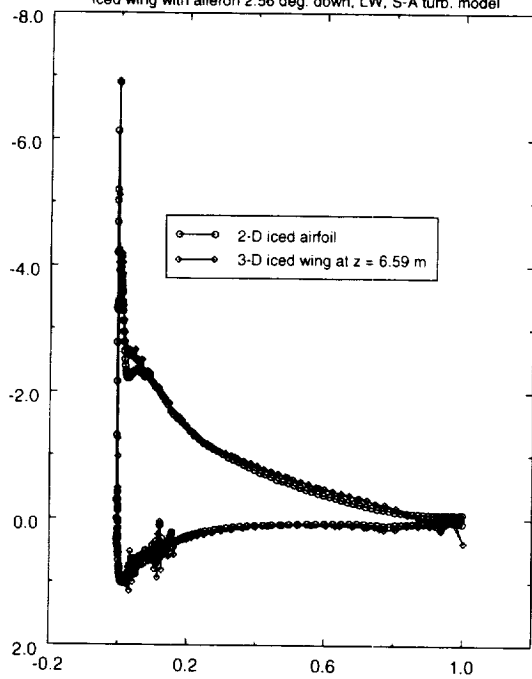
Fig. 17a Rake profile for 3-D wing at AOA = 13 deg.
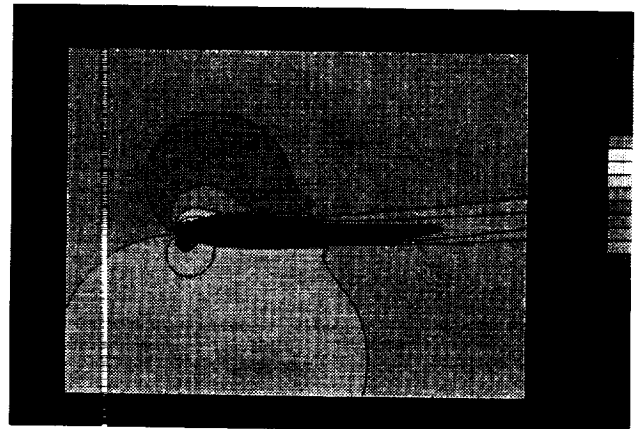
Fig. 17b Mach contour at AOA = 13 degrees

Fig. 18 Cp change due to various AOA for 3-D iced wing

Aileron down 2.56 deg. LW, S-A turb. model, at z = 6.59 m

Legend:
- AOA = 9 deg.
- AOA = 11 deg.
- AOA = 13 deg.
- AOA = 15 deg.
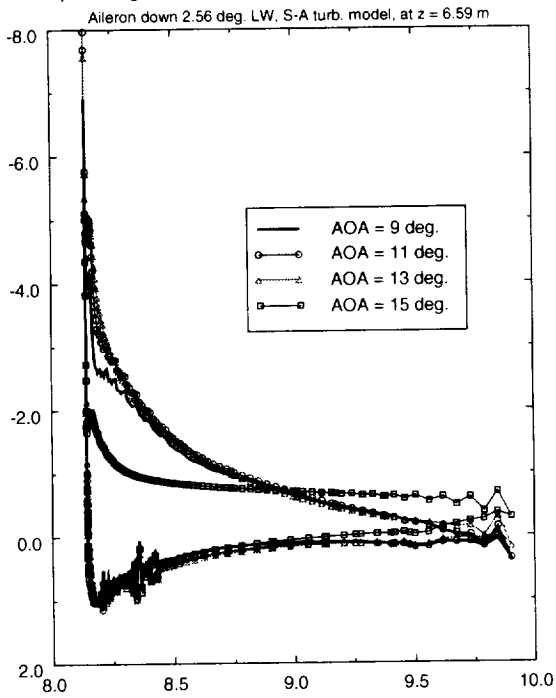
Fig. 19a Cp distribution in spanwise direction for 3-D iced wing

AOA = 13 deg., aileron at z = 6.3 ~ 9.6 m

Legend:
- Lower surface, near the aileron hinge
- At the trailing edge
- Upper surface near the aileron hinge
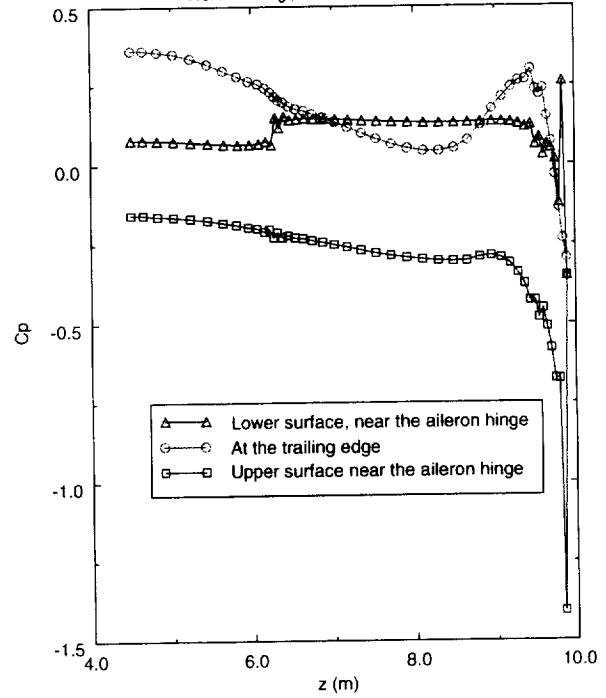
Fig. 19b Cp distribution in spanwise direction for 3-D iced wing

AOA = 15 deg., aileron at z = 6.3 ~ 9.6 m

Legend:
- Lower surface, near the aileron hinge
- At the trailing edge
- Upper surface near the aileron hinge
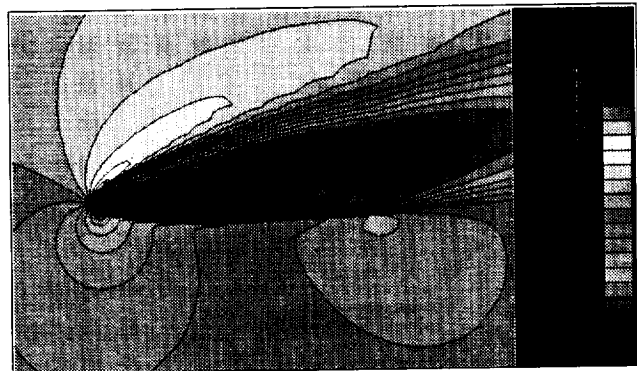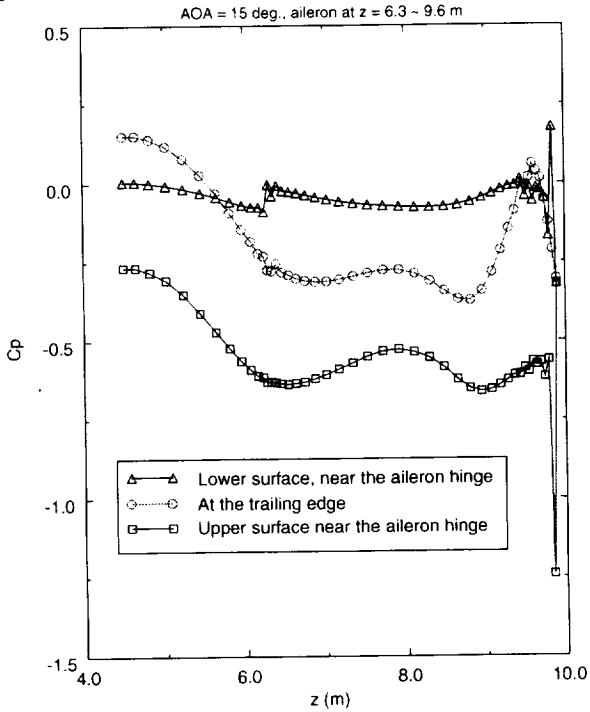
Fig. 20a Mach contour at AOA = 15 degrees
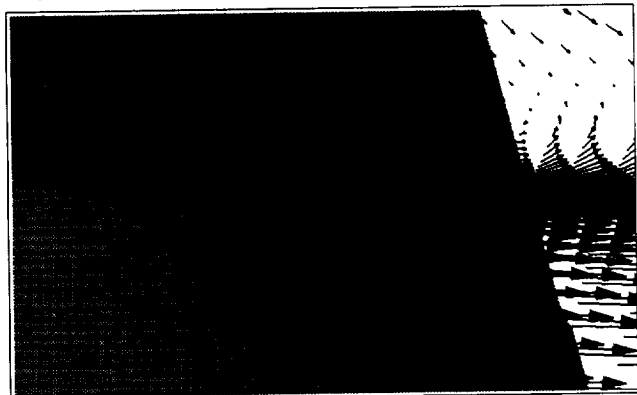
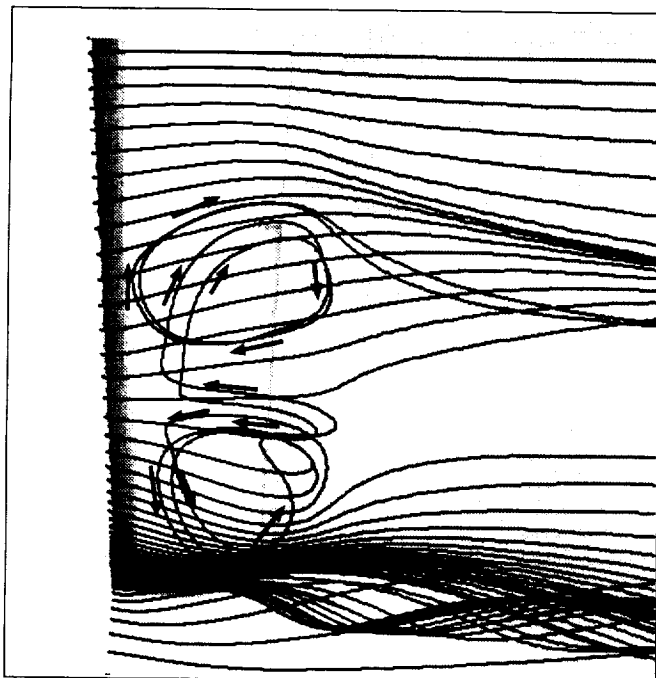Fig. 20b Trailing edge separation near the wing tip.

17

Fig. 21 Circular flow pattern on the upper surface of the iced wing appearing at AOA = 15 degrees

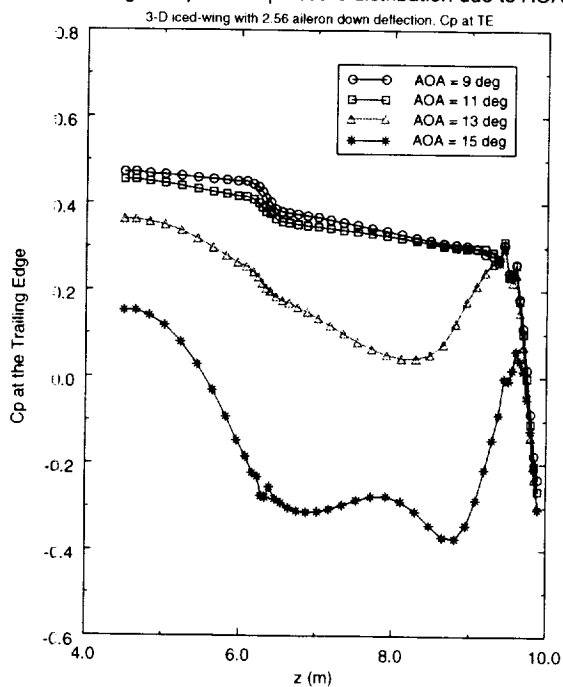Fig. 22 Change of spanwise pressure distribution due to AOA

3-D iced-wing with 2.56 aileron down deflection. Cp at TE
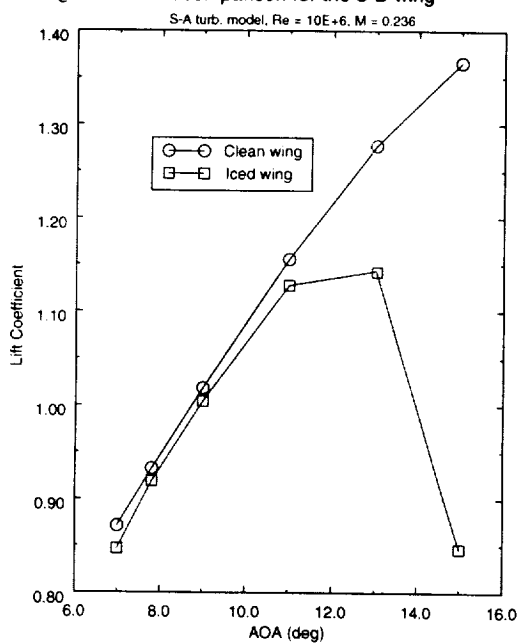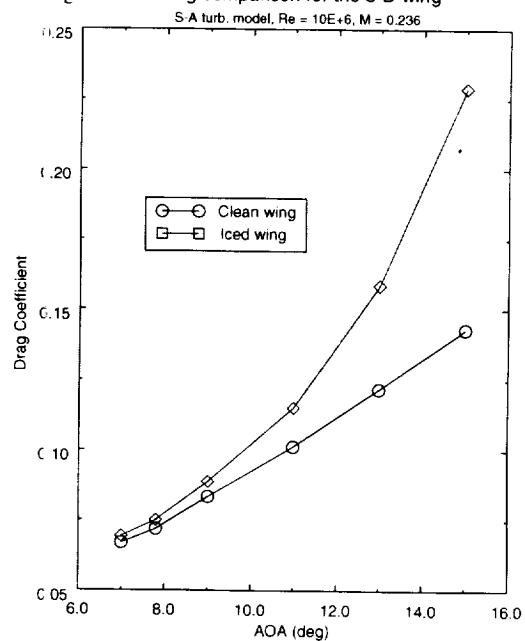
Fig. 23 Lift comparison for the 3-D wing

S-A turb. model, Re = 10E+6, M = 0.236

Fig. 24 Drag comparison for the 3-D wing

S-A turb. model, Re = 10E+6, M = 0.236

REPORT DOCUMENTATION PAGE

Form Approved
OMB No. 0704-0188

1. AGENCY USE ONLY (Leave blank)	2. REPORT DATE	3. REPORT TYPE AND DATES COVERED
	January 1999	Technical Memorandum

4. TITLE AND SUBTITLE

Navier-Stokes Analysis of the Flowfield Characteristics of an Ice Contaminated Aircraft Wing

5. FUNDING NUMBERS

WU–548–20–23–00

6. AUTHOR(S)

J. Chung, Y. Choo, A. Reehorst, M. Potapczuk, and J. Slater

7. PERFORMING ORGANIZATION NAME(S) AND ADDRESS(ES)

National Aeronautics and Space Administration
Lewis Research Center
Cleveland, Ohio 44135–3191

8. PERFORMING ORGANIZATION REPORT NUMBER

E–11496

9. SPONSORING/MONITORING AGENCY NAME(S) AND ADDRESS(ES)

National Aeronautics and Space Administration
Washington, DC 20546–0001

10. SPONSORING/MONITORING AGENCY REPORT NUMBER

NASA TM—1999-208897
AIAA–99–0375
ICOMP–99–03

11. SUPPLEMENTARY NOTES

12a. DISTRIBUTION/AVAILABILITY STATEMENT

Unclassified - Unlimited
Subject Categories: 02 and 03

Distribution: Nonstandard

This publication is available from the NASA Center for AeroSpace Information, (301) 621–0390.

12b. DISTRIBUTION CODE

13. ABSTRACT (Maximum 200 words)

An analytical study was performed as part of the NASA Lewis support of a National Transportation Safety Board (NTSB) aircraft accident investigation. The study was focused on the performance degradation associated with ice contamination on the wing of a commercial turbo-prop-powered aircraft. Based upon the results of an earlier numerical study conducted by the authors, a prominent ridged-ice formation on the subject aircraft wing was selected for detailed flow analysis using 2-dimensional (2-D), as well as, 3-dimensional (3-D) Navier-Stokes computations. This configuration was selected because it caused the largest lift decrease and drag increase among all the ice shapes investigated in the earlier study. A grid sensitivity test was performed to find out the influence of grid spacing on the lift, drag, and associated angle-of-attack for the maximum lift ($C_{l_{max}}$). This study showed that grid resolution is important and a sensitivity analysis is an essential element of the process in order to assure that the final solution is independent of the grid. The 2-D results suggested that a severe stability and control difficulty could have occurred at a slightly higher angle-of-attack (AOA) than the one recorded by the Flight Data Recorder (FDR). This stability and control problem was thought to have resulted from a decreased differential lift on the wings with respect to the normal loading for the configuration. The analysis also indicated that this stability and control problem could have occurred whether or not natural ice shedding took place. Numerical results using an assumed 3-D ice shape showed an increase of the angle at which this phenomena occurred of about 4 degrees. As it occurred with the 2-D case, the trailing edge separation was observed but started only when the AOA was very close to the angle at which the maximum lift occurred.

14. SUBJECT TERMS

Aircraft icing; Computational fluid dynamics; Aerodynamic characteristics

15. NUMBER OF PAGES
24

16. PRICE CODE
A03

17. SECURITY CLASSIFICATION OF REPORT	18. SECURITY CLASSIFICATION OF THIS PAGE	19. SECURITY CLASSIFICATION OF ABSTRACT	20. LIMITATION OF ABSTRACT
Unclassified	Unclassified	Unclassified	